Materials Science and Engineering A 525 (2009) 1–6

Contents lists available at ScienceDirect

Materials Science and Engineering A

journal homepage: www.elsevier.com/locate/msea

Compressive properties of a closed-cell aluminum foam as a function of strain rate and temperature

C.M. Cady[a,*], G.T. Gray III[a], C. Liu[a], M.L. Lovato[a], T. Mukai[b]

[a] Los Alamos National Laboratory, Los Alamos, NM 87545, United States
[b] National Institute for Material Science, Tsukuba, Ibaraki 305-0047, Japan

ARTICLE INFO

Article history:
Received 23 December 2008
Received in revised form 18 March 2009
Accepted 2 July 2009

Keywords:
Aluminum foam
High-strain rate
Closed-cell foam

ABSTRACT

The compressive constitutive behavior of a closed-cell aluminum foam (ALPORAS) manufactured by Shinko Wire Co. in Japan was evaluated under static and dynamic loading conditions as a function of temperature. High-strain-rate tests (1000–2000 s^{-1}) were conducted using a split-Hopkinson pressure bar (SHPB). Quasi-static and intermediate-strain-rate tests were conducted on a hydraulic load frame. A small but discernable change in the flow stress behavior as a function of strain rate was measured. The deformation behavior of the Al-foam was however found to be strongly temperature dependent under both quasi-static and dynamic loading. Localized deformation and stress state instability during testing of metal foams is discussed in detail since the mechanical behavior over the entire range of strain rates indicates non-uniform deformation. Additionally, investigation of the effect of residual stresses created during manufacturing on the mechanical behavior was investigated.

1. Introduction

The high-strain-rate stress–strain response of metallic foams has received increased interest in recent years related to their lightweight and the potential for large energy absorption during deformation. Understanding the deformation mechanisms present in these materials will enable designers to more fully utilize their energy absorbing characteristics. Previous studies of fully dense annealed Al alloys have shown that temperature more strongly affects the yield and flow stress behavior than strain rate [1].

A number of previous studies have probed the constitutive response of aluminum-based foams at room temperature [2–27]. Research results by Aly [27] and Hakamada et al. [28] describe the elevated temperature response of aluminum foam and limited studies on the effect of heat treatment [2,3]. The room temperature compressive response of a variety of Al-based foams at low-strain rates [4–10] and under dynamic loading conditions [3,10–24] has shown that: (a) the initial elastic modulus of Al-foams is generally lower than a fully dense alloy, (b) imperfections in the cell walls [4,9,29] lead to localized deformation, stress concentrations around the deformed regions, and due to this a decreased elastic modulus, (c) Al-foams exhibit yield behavior when the local distortions link to form deformation bands, and (d) subsequent oscillations in the stress–strain curves of Al-foams tested in compression are associated with additional deformation band collapse.

Deformation of metallic foams is typically divided into three stages (Fig. 1): a linear elastic deformation stage, a plastic deformation and pore collapse stage, and finally a densification stage [20]. The linear elastic stage of the deformation has been shown to be related to elastic bending of the cell walls. Studies have demonstrated that there are weak regions in Al-foam materials due to the inhomogeneous density of the closed-cell foams [4,9,29]. At low-strain rates the pore collapse stage consists of an initial load drop due to local buckling and failure of the wall structure on a plane normal to the loading direction at the weakest region of the sample. Stresses in the collapse plane will increase as the cell walls interact with one another until the load level reaches a value where the next plane of failure will occur. Additional pore collapse planes will occur randomly across the sample at the same time as there is continued cell wall interaction in the original and subsequent layers reducing the magnitude of oscillations seen in the stress–strain curves due to a plane of pore collapse. At high-strain rates, strain rates high enough to cause inertial effects, the mechanism of plastic deformations has been seen to be quite different [18,22,23,25,26]. The collapse planes are no longer randomly found within the sample but plastic deformation occurs as a sweeping deformation front starting from the impact surface and propagating across the sample. This reinforces the findings of authors that observed strain-rate effects in these materials [12–15,17,20–26]. Finally, the densification stage shows a rapid increase in the load carried by the sample.

* Corresponding author at: Los Alamos National Laboratory, Materials Science and Technology, MST-8 MS G755, Los Alamos, NM 87545, United States.
Tel.: +1 505 667 6369; fax: +1 505 667 8021.
E-mail address: cady@lanl.gov (C.M. Cady).

0921-5093/$ – see front matter © 2009 Published by Elsevier B.V.
doi:10.1016/j.msea.2009.07.007

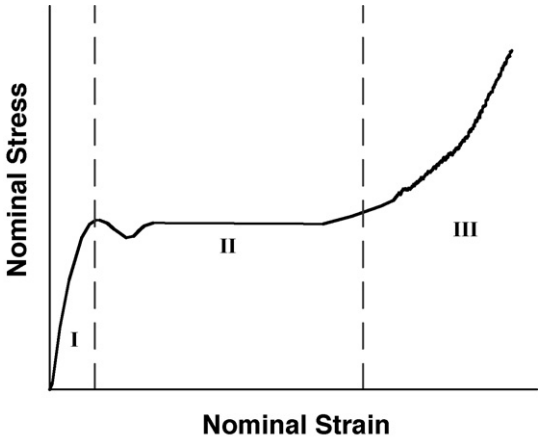

Fig. 1. A typical stress–strain curve for metal foam deformation showing stage I, linear elastic "bending", stage II, pore collapse, buckling, and cell wall failure, and stage III, densification.

Although these summary observations are common to the findings of most previous investigators, there remain significant differences in interpretation concerning the nature and rate controlling mechanisms of the strain-rate sensitivity of Al-alloy foams. There is evidence that the stress–strain behavior of the closed-cell Al-foam (Alporas) used in this study exhibits some strain-rate sensitivity. One theory is that gas entrapment, reduced or restricted air flow, influences the strain-rate sensitivity of these materials [10,11,15,26]. An additional theory suggests that gas entrapment does not influence the mechanical behavior but the rate sensitivity is associated with cell structure, orientation, density and base material properties [3,12–15,17,20,21,23,24,26]. Subsets of the latter theory associates the rate sensitivity to microinertial effects [17,22,23,26], uniform ordered structures versus random [12,14,20,21,24], and fracture versus folding or bending of the cell structure [24,26], but the most prevalent theory for rate sensitivity in Al-foam materials is that if the base materials display a rate sensitivity then the low density foam of the same material will also be rate sensitive [3,12–15,22,23,26]. Other studies have concluded that there is no strain-rate sensitivity in metal foams [8–12,16,19]. However, there has been to date no evidence linking strain-rate sensitivity to processing. There does appear to be some strengthening of the metal foams due to residual stresses produced during manufacturing. As part of this investigation annealed samples were interrogated under similar conditions as the as-processed Al-foam material. Analysis of the energy absorption will be presented in this study to help quantify the magnitude of the strain-rate sensitivity of the aluminum foam characterized in this study.

A potential previously postulated contributor to the strain-rate sensitivity of closed-cell aluminum foam is that of compressing the trapped gas, assuming that the cell walls do not fracture during pore collapse. However, it has been shown that the contribution to the strength due to gas compaction is negligible [12,22]. The calculated increase in strength will be nearly zero at low-strain rates and at higher strain rates the contribution typically less that about 5% of the yield stress and as such falls within the scatter for the experiments.

Sample size and lubrication effects are also critical to the quantification of the mechanical response of metal foams due to the cell size, cell wall thickness, and the speed of sound through these structures. The speed of sound in Al-foam structures, which is linked to the stress state stability in dynamic SHPB tests, seems to vary with wall geometry and pore size.

The objective of this paper is to present results illustrating the effect of systematic variations of strain rate and temperature on the constitutive response of Alporas closed-cell Al-foam.

2. Experimental techniques

This investigation was performed on a commercial closed-cell aluminum alloy foam with the trade name ALPORAS (Shinko Wire Co.) [30]. The chemical composition of the foam is Al–1.42Ca–1.42Ti–0.28Fe–0.007Mg (by weight %) with an approximate relative density of 0.08 (density of foam divided by the density of the parent material). The average cell dimension of this foam is ~3.0 mm in the in plane orientation and ~3.8 mm in the through thickness orientation [30]. The effect of orientation will not be presented in this study as it has been investigated previously [22] and showed only minor differences for metal foams with similar cell structures. The cell wall thickness is reported to be ~85 μm in the center of a web and thickens nearer the intersection of three or more cells. There are morphological defects like cell wall waviness, cell size variation, fractured cell walls, and non-uniform cell wall thickness that are present in all of the foam specimens.

Cylindrical compression samples 18.4 mm in diameter by 9.5 mm in length (high rate tests) and 25.3 mm in diameter by 28.0 mm in length or 22.8 mm width by 22.8 mm thick by 30.2 length (low rate tests) were electro-discharge machined from the as-received foam material. Several samples were subsequently annealed at 373 K for 2 h. It was hoped that this low tempera-

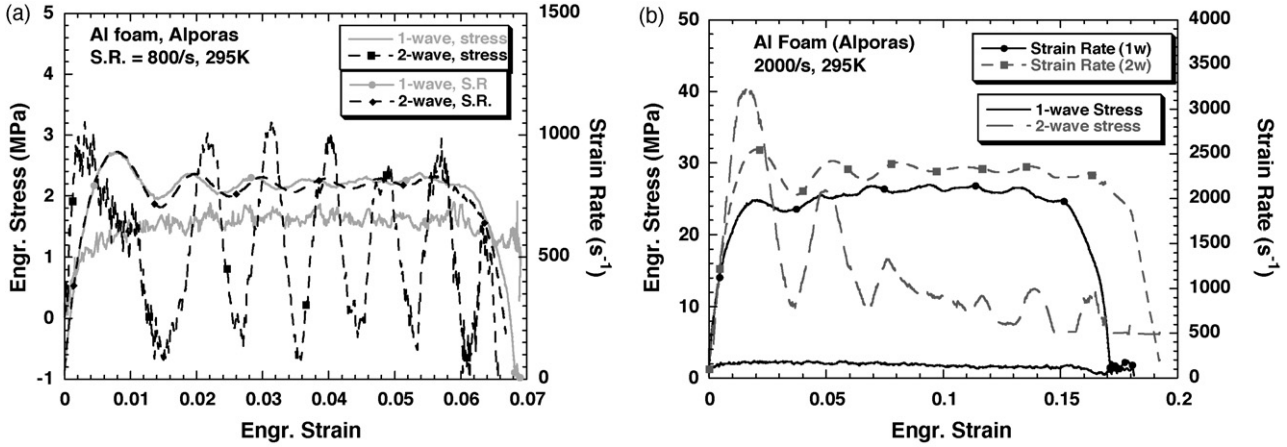

Fig. 2. Stress–strain response the Al-foam showing 1-wave and 2-wave stress curves in addition to the strain rate for (a) a test with a strain rate of 800 s^{-1} where the 2-wave stress oscillates about the 1-wave stress indicating a valid test for incompressible materials, and (b) showing 1-wave and 2-wave stress curves at 2000 s^{-1} where the 1-wave and 2-wave stress curves are divergent.

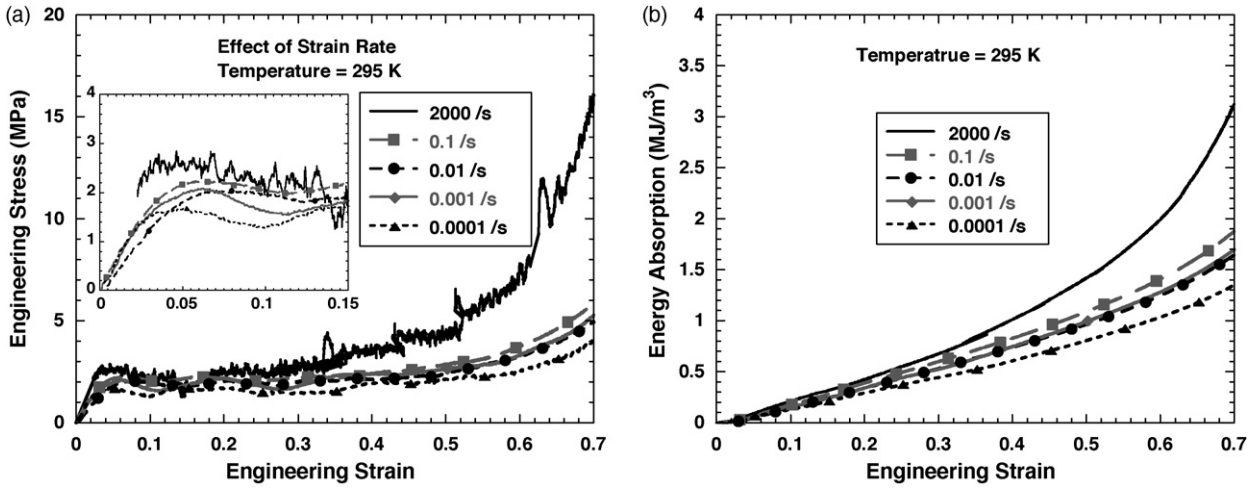

Fig. 3. Room temperature response of Alphoras Al-foam (relative density = 0.08) as a function of strain rate: (a) stress–strain response and (b) energy absorption.

ture anneal would relieve any residual stresses introduced into the material during the manufacturing of the base material or the machining of the test samples. Compression tests were conducted at strain rates of 0.001 and 1.0 s^{-1} at 77, 173, and 295 K in laboratory air using an MTS 880 hydraulic load frame. A minimum of three tests were conducted for each test condition and the curve that best represented the average properties is presented in the plots. Dynamic tests were conducted at strain rates from ~1000 to 2000 s^{-1}, and at temperatures of 77, 173, and 295 K, utilizing a split-Hopkinson pressure bar (SHPB) equipped with 23 mm diameter AZ31B magnesium pressure bars. Mg bars were utilized as they offer a higher signal-to-noise level, due to their reduced elastic modulus, compared to the maraging steel bars traditionally utilized in many Hopkinson–Bar studies [31]. A valid, uniaxial Hopkinson bar test requires that (1) the stress state throughout the sample achieve equilibrium, (2) a constant strain rate must be demonstrated, and (3) volume must be conserved [31]. These requirements will be further elaborated in the discussion in the context of the interpretation of the high-strain-rate Al-foam mechanical property response. Hopkinson bar experiments showing large strains were generated by multiple loadings using strain limiting rings to sequentially control the deformation in each increment of loading in the Al-foam sample. Without the rings, the stored energy in the SHPB leads to deformation in the samples well beyond the recording ability of the data acquisition system. At least three tests were run for each test condition and the curve that best represented the average properties was selected for the plots.

The inherent oscillations in the dynamic stress–strain curves and the lack of stress equilibrium in the specimens during the test make the determination of yield strength inaccurate at high-strain rates. Cryogenic temperature tests were conducted by immersing the sample in a liquid nitrogen bath. The 173 K temperature condition for the quasi-static tests was achieved by allowing cooled nitrogen gas to flow through the compression platens utilized for these tests. SHPB tests at 173 K were achieved by passing cold nitrogen gas over a sample and the SHPB bars and allowing the system to equilibrate. Because it is well known that the base material of the foam is more sensitive to temperature than strain rate it was believed that characterizing the material at low temperatures could lead to insights that might otherwise be missed. The test samples were lubricated using either a thin layer of molybdenum disulfide grease or molybdenum disulfide spray lubricant to reduce friction effects at the sample-load frame interface.

3. Results and discussion

3.1. SHPB characterization

The determination of the stress–strain behavior of a material being tested utilizing a split-Hopkinson pressure bar (SHPB) is based on the principle of one-dimensional elastic-wave propagation within the pressure bars and the attainment of a uniaxial-stress state in the sample of interest [31]. Due to the documented deformation characteristics of these closed-cell foams [22,23,26], i.e., non-uniform plasticity, the data generated in a SHPB studies is ill posed based on the requirements for valid uniaxial-stress SHPB experiments [31,32]. A uniform uniaxial-stress state and homogeneous deformation within a sample, which is essential for valid SHPB tests, is seen to be problematic at best within this material at strain rates of 0.001 s^{-1} and above due to non-uniform deformation of the foams. Further, the non-conservancy of volume, i.e., the sample is compressible, eliminates the possibility of determining true-stress true-strain data. Nevertheless, the high-rate constitutive response of the Al-foam in this study was carefully quantified to identify the high-rate mechanical response of the foam as a means to assess its energy absorption response under dynamic loading.

Additionally, to assure that valid high-rate measurements on the Al-foam were being measured, it is instructive to examine the different wave analyses [31,33] used to calculate sample stress using the incident, reflected, and transmitted bar strains measured in a SHPB as shown in Fig. 2a. In the 1-wave analysis the sample stress is directly proportional to the bar strain measured in the transmitted bar. The 1-wave stress analysis reflects the conditions at the sample-transmitted bar interface and is often referred to as the sample "back stress". This analysis results in smoother stress–strain curves, especially near the yield point. Alternatively in a 2-wave analysis, the sum of the synchronized incident and reflected bar waveforms (which are opposite in sign) is proportional to the sample "front stress" and reflects the conditions at the incident/reflected bar-sample interface.

A valid, uniaxial-stress Hopkinson bar test requires that the stress state throughout the sample achieve equilibrium during the test and this condition can be checked readily by comparing the 1-wave and 2-wave stress–strain responses [31,33]. We know from the observed deformation of the Al-foam samples that the deformation within the samples is not uniform and therefore neither can the achievement of stress-state equilibrium within the sample. Since the 2-wave stress analysis oscillates about the 1-wave wave stress

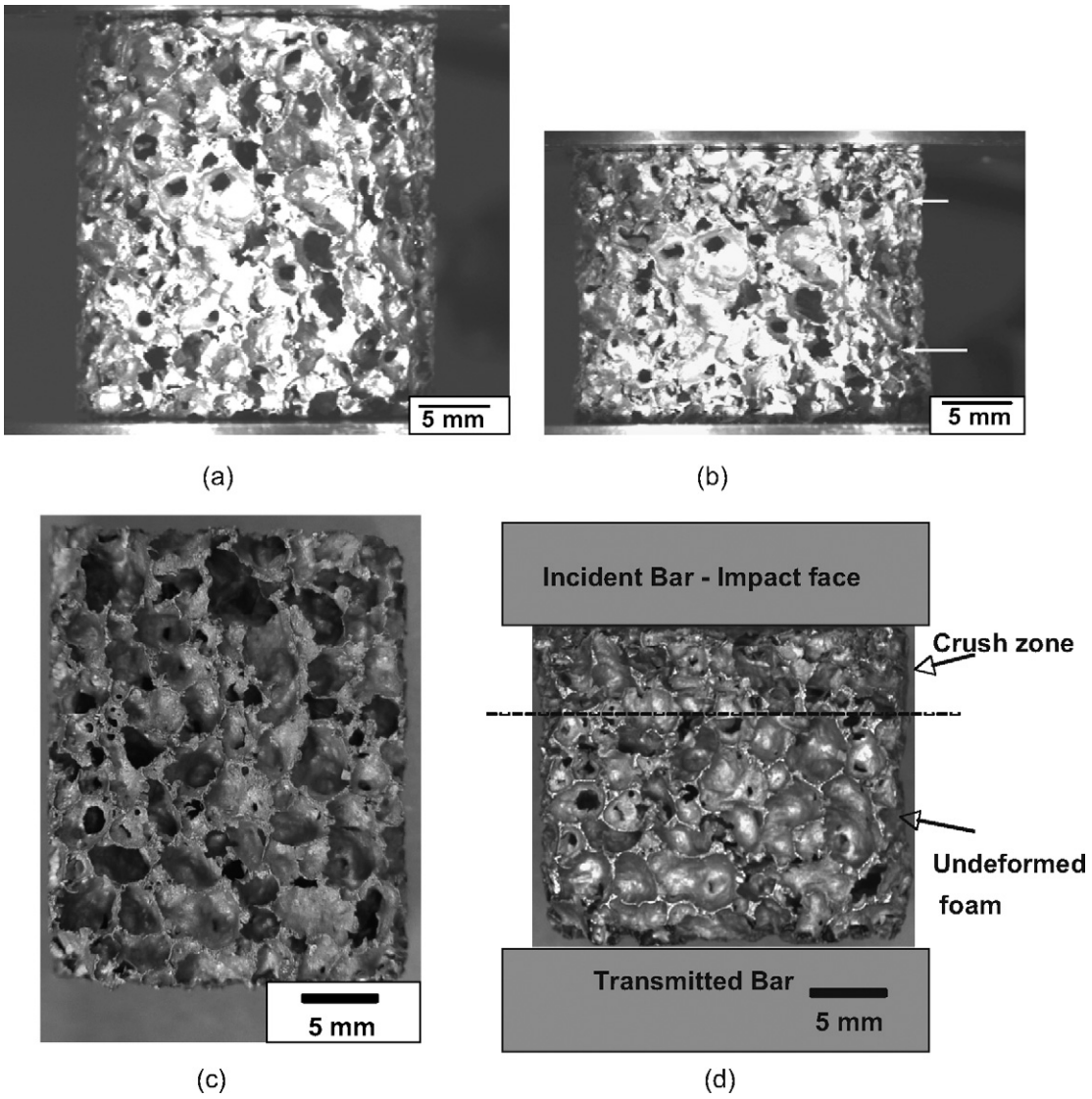

Fig. 4. Optical micrograph of Alporas Al-foam under quasi-static and high-strain-rate loading: (a) as-received, low-strain-rate sample, (b) after 30% strain at 0.001 s^{-1} note the deformation bands indicated by the arrows, (c) as-received, high-strain-rate sample and (d) high-strain rate (~2000 s^{-1}) sample with ~32% strain showing advancing deformation front.

at a strain rate of ~800 s^{-1}, as seen in Fig. 2a we have some confidence that the forces measured represent the overall "bulk" loads on the Al-foam samples. However, at the strain rate of ~1800 s^{-1} the 1-wave and 2-wave signals were found to be divergent at the beginning of each test and the strain rate is seen to slightly increase with plastic strain. Although the 2-wave data oscillates around the 1-wave curve there is sufficient evidence to therefore seriously question the validity of these SHPB results. At even higher strain rates, or impact velocities, the 1-wave and 2-wave wave analyses were found to be divergent for the entire test (Fig. 2b) likely indicating non-equilibrium deformation for the entire duration of the test and accordingly indicating these SHPB tests were ill posed. Even though these tests are invalid based upon the traditional SHPB data analysis, it is believed that the results can be utilized qualitatively to provide insight into the deformation behavior of the Al-foam material under impact loading. However, the reader is advised to not expect the reported values for the high-strain-rate data to be exact or consistent from one experimentalist to another given this ill posed state and lack of stress-state stability within the samples. Depending on the configuration of the SHPB system used, the impact velocities can be different yet produce the same strain rate based on variables including sample size, bar diameter, and bar material.

3.2. Compressive response and energy absorption

The compressive engineering-stress versus engineering-strain response of the Alphoras Al-foam was found to be sensitive to the applied strain rate between 0.0001 and 2000 s^{-1}. The plateau stresses were found to be parallel with a small average increase in level for increasing strain rate. The yield strength and plateau flow stress displayed greater dependence on temperature between 77 and 295 K. The plateau strength of the foam at 295 K, shown in Fig. 3a, increased from ~1.6 MPa at 0.0001 s^{-1} to 1.96 MPa at 0.1 s^{-1} to ~2.5 MPa at a strain rate of 2000 s^{-1}. However, tests above a strain rate of 1700 s^{-1} are complicated, as discussed above, by non-uniform deformation and the lack of attainment of a uniaxial state of stress. The result of the 900 s^{-1} test shows a yield of only ~1.7 MPa, but it exhibits a more uniform state of stress within the sample during dynamic testing. Since the 1-wave stress reflects the transmitted force from the foam specimen to the transmitted bar at the contact end, the absorption energy per unit volume, W, at a specific strain

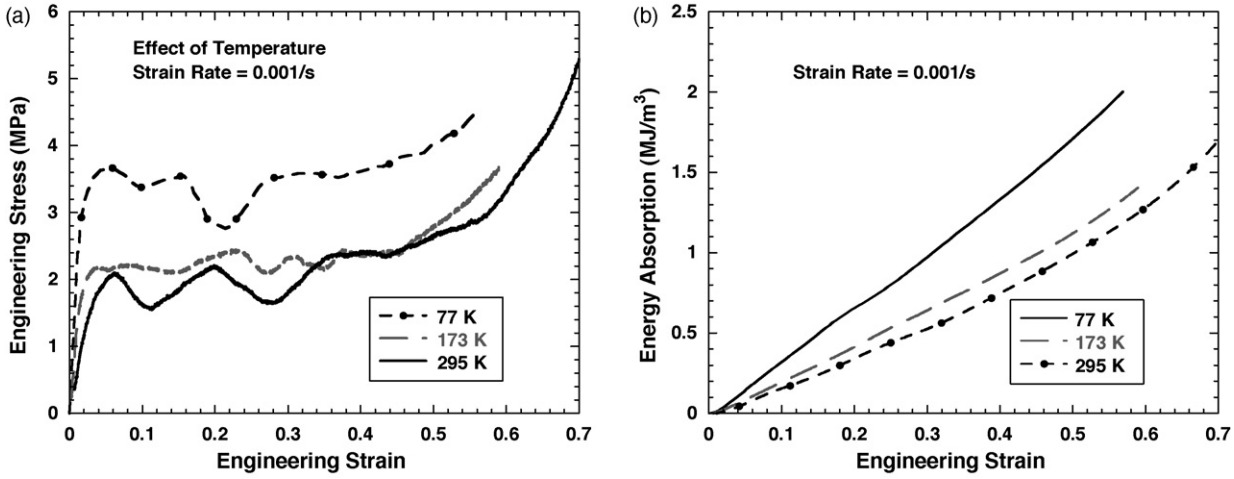

Fig. 5. Temperature response of Alphoras Al-foam (relative density = 0.08) at a strain rate of 0.001 s^{-1}: (a) stress–strain response and (b) energy absorption.

can be evaluated by integrating the area under the stress–strain curve by 1-wave analysis as given by

$$W = \int_0^{\varepsilon} \sigma \, d\varepsilon \tag{1}$$

For all the samples tested in this study the energy absorbed was found to monotonically increase with plastic strain until the material showed signs of densification. An engineering strain of 0.5 was chosen as the evaluation point because it is near the transition of the pore collapse regime and the densification regime. The absorbed energy ranged from 1.0 to 1.1 MJ/m^3 for strain rates between 0.001 and 0.1 s^{-1} and it went to 1.44 at 2000 s^{-1} (Fig. 3b). There was a significant change in the absorbed energy between the quasi-static (0.001 s^{-1}) and the dynamic rate (~1000 s^{-1}). It is interesting to note that there is a marked increase in the energy absorption above a strain rate of ~1000 s^{-1}. Micrographs of the different pore collapse phenomenon are illustrated in Fig. 4. The undeformed samples for low and high-strain rates are shown in Fig. 4a and c, respectively. The planes of spatially random pore collapse for low-strain rate experiments (~0.001 s^{-1}) are highlighted with arrows in Fig. 4b. The micrograph of high-strain-rate deformation, on the order of ~2000 s^{-1}, shows that over 90% of the deformation observed is found in the first 30% of the sample (Fig. 4d). This is the expected deformation behavior for a foam material that exhibits divergent 1-wave and 2-wave stress–strain behavior. The calculated engineering strain in the highly deformed region is ~64% and if one refers to Fig. 3a one notices that this is where the stress in the material dramatically increase due to complete pore collapse and densification. The marked increase in the energy absorption at high-strain rate may correlate with the transition from spatially random pore collapse planes to the propagation of the failure from the impact surface in a sweeping wave front manner.

The plateau stress of the Al-foam studied was found to additionally exhibit a dependence on test temperature, decreasing from ~2.4 MPa at 77 K to 1.85 MPa at 295 K, a 29% change, when loaded at a strain rate of ~1000 s^{-1}. A similar effect of temperature on the stress–strain response of the Al-foam was seen during quasi-static testing as seen in Fig. 5a. The plateau stress exhibited a much more pronounced decreased from ~3.4 MPa at 77 K to ~1.8 MPa at 295 K, an 89% change. This temperature dependency of the Al-foam is thought to reflect the temperature dependence of the pre-existing defect substructure, stored dislocations, formed during the manufacturing process [34]. The effect of cooling the material on energy absorption for tests conducted at 0.001 s^{-1} is ~1.0 MJ/m^3 at 295 K, ~1.1 MJ/m^3 at 173 K and ~1.7 MJ/m^3 at 77 K (Fig. 5b), a 70% increase relative to the room temperature behavior.

This study also sought to quantify the effect of residual stresses and/or stored cold-work in the Al-foam samples created during the foaming process. Al-foam samples were heat treated for 1 h at 373 K

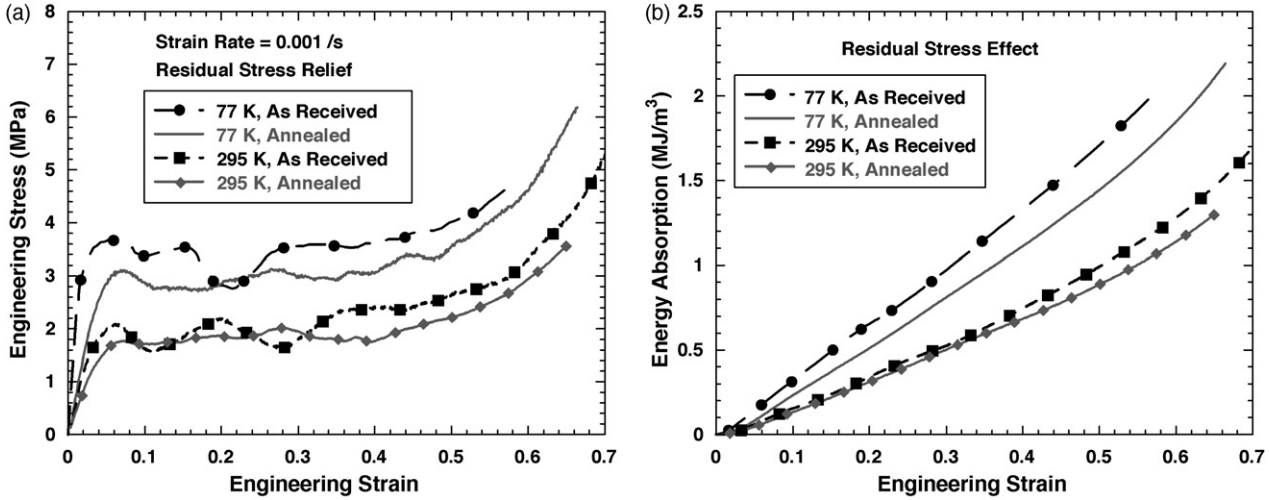

Fig. 6. Effect of annealing as a function of temperature at a strain rate of 0.001 s^{-1}: (a) stress–strain response and (b) energy absorption.

and were subsequently evaluated at similar strain rate and temperature testing conditions as those for the as-received material. The stress–strain behavior and absorbed energy for the annealed Al-foam material are presented in Fig. 6. The subtle decrease in flow stress response suggests the presence of either some level of residual stresses and/or cold-work in the material that has been annealed out by the low temperature thermal soak. The plateau stress was found to be reduced by an average of ~0.5 MPa at 77 K and ~0.15 MPa at 295 K. The energy absorption (Fig. 6b) reflects this variation clearly with a difference of nominally 0.25 MJ/m^3 at 77 K and 0.11 MJ/m^3 at room temperature.

Finally, the Al-foam samples each displayed strain-rate sensitivity with respect to the densification process during testing. The primary difference between the two loading-rate responses is seen in the strain at which the buckling bands have saturated and "bulk" densification initializes, where the stress begins to increase after the plateau (at ~63% strain in the low-strain rate tests and at ~51% for strain rates of 10^3). In addition, there is also the mechanism governing pore collapse, i.e., random versus a sweeping deformation front, as discussed previously.

4. Summary and conclusions

The strength properties of the ALPORAS aluminum foam with a relative density of 0.08 has been characterized and its response to quasi-static and dynamic loading at various temperatures presented. The initial pore collapse, plateau stress, and densification have been described with the energy absorption calculated form the resultant curves.

It was found that there is a regime where the impact velocity or applied strain rate was high enough to produce localization of the crushing and increase the strength of the foam by allowing inertial effects to dominate the deformation behavior. At these "super-critical" strain rates specimen size, cell structure, and defects become insignificant. Post-impact examination of partially crushed specimens showed that deformation for these super-critical strain rates propagated by progressive cell crushing from the impact surface. For all lower strain rates deformation is through the cumulative interaction of discrete crush bands that are dominated by statistical strength properties of the foam. The onset of "super-critical" dynamic deformation is likely linked to pore and wall geometry, foam density, and morphological defects and is not a material constant. Increased strain-rate sensitivity is likely due to cell wall interaction and pore architecture as well as the inherent rate sensitivity of the base metal of the foam material.

These results are consistent with previous strain-rate studies on cellular aluminum alloys considering the statistical variation in the material [3,7–26].

A significant influence on the strength of the material when exposed to low temperatures was observed. The quasi-static loading of the foam material showed the greatest strength increase of all conditions. Part of the rationale behind this response is thought to be that at high loading rates adiabatic heating at a local level can be very high, and since the deformation is propagating through the sample from the impact surface into the sample the local temperatures in the foam materials could be several 10's if not more than a 100° warmer at the point of deformation thus allowing the material to deform at a lower flow stress level. It was also observed that low temperature annealing reduced the stress at which deformation initiated indicating that the material has some residual stresses and/or cold-work introduced during fabrication of the foam material.

Based upon a study of the influence of strain rate and temperature on the constitutive response of Al-foams, the following conclusions can be drawn: (1) the compressive stress–strain response of an Al-foam was found to depend on the applied temperature; 77–295 K and to a lesser degree on the strain rate; 0.001 to ~2000 s^{-1}, (2) decreasing temperature at 2000 s^{-1} was found to increase the maximum flow stress in Al-foam from ~1.4–4 MPa, (3) the deformation of the Al-foam was found to be heterogeneous in nature, (4) the Al-foam failed at high-strain rate via deformation band collapse and (5) there appear to be residual stresses in the as-processed Al-foam materials that can be relieved by a low temperature anneal.

Acknowledgements

Los Alamos National Laboratory is operated by LANS, LLC, for the National Nuclear Security Administration of the U.S. Department of Energy under contract DE-AC52-06NA25396. This work has been performed under the auspices of the United States Department of Energy and was supported by the Joint DoD/DOE Munitions Technology Development Program.

References

[1] J.E. Hockett, AIME Trans. 239 (1967) 969–976.
[2] X.Q. Cao, Z.H. Wang, H.W. Ma, L.M. Zhao, G.T. Yang, Trans. Nonferrous Met. Soc. China 16 (1) (2006) 159–163.
[3] H. Kanahashi, T. Mukai, Y. Yamada, K. Shimojima, M. Mabuchi, T. Aizawa, K. Higashi, Mater. Trans. 42 (10) (2001) 2087–2092.
[4] Y. Sugimura, M. Meyer, M.Y. He, H. Bart-Smith, J. Grenstedt, A.G. Evans, Acta Mater. 45 (12) (1997) 5245–5259.
[5] A.-F. Bastawros, H. Bart-Smith, A.G. Evans, J. Mech. Phys. Solids 48 (2000) 301–322.
[6] O.B. Olurin, N.A. Fleck, M.F. Ashby, Mater. Sci. Eng. A 291 (2000) 136–146.
[7] T. Miyoshi, M. Itoh, T. Mukai, H. Kanahashi, H. Kohzu, S. Tanabe, K. Higashi, Scripta Mater. 41 (10) (1999) 1055–1060.
[8] D. Ruan, G. Lu, F.L. Chen, E. Siores, Compos. Struct. 57 (2002) 331–336.
[9] H. Yu, Z. Gao, B. Li, G. Yao, H. Lou, Y. Liu, Mater. Sci. Eng. A 454/455 (2007) 542–546.
[10] R. Montanini, Int. J. Mech. Sci. 47 (2005) 26–42.
[11] K.A. Dannemann, J. Lankford Jr., Mater. Sci. Eng. A 293 (2000) 157–164.
[12] V.S. Deshpande, N.A. Fleck, Int. J. Impact Eng. 24 (2000) 277–298.
[13] T. Mukai, H. Kanahashi, T. Miyoshi, M. Mabuchi, T.G. Nieh, K. Higashi, Scripta Mater. 40 (8) (1999) 921–927.
[14] H. Kanahashi, T. Mukai, Y. Yamada, K. Shimojima, M. Mabuchi, T.G. Nieh, K. Higashi, Mater. Sci. Eng. A 280 (2000) 339–353.
[15] T. Mukai, T. Miyoshi, S. Nakano, H. Somekawa, K. Higashi, Scripta Mater. 54 (2006) 533–537.
[16] I.W. Hall, M. Guden, C.-J. Yu, Scripta Mater. 43 (2000) 515–521.
[17] A. Paul, U. Ramamurty, Mater. Sci. Eng. A 281 (2000) 1–7.
[18] N.K. Bourne, K. Bennett, A.M. Milne, S.A. MacDonald, J.J. Harrigan, J.C.F. Millett, Scripta Mater. 58 (2008) 154–157.
[19] J.-L. Yu, X. Wang, Z.-G. Wei, E.H. Wang, Int. J. Impact Eng. 28 (2003) 331–347.
[20] J.-L. Yu, J.R. Li, S.S. Hu, Mech. Mater. 38 (2006) 160–170.
[21] W. Zhihua, M. Hongwei, Z. Longmao, Y. Guitong, Scripta Mater. 54 (2006) 83–87.
[22] P.J. Tan, J.J. Harrigan, S.R. Reid, Mater. Sci. Technol. 18 (2002) 480–488.
[23] P.J. Tan, S.R. Reid, J.J. Harrigan, Z. Zou, S. Li, J. Mech. Phys. Solids 53 (2005) 2174–2205.
[24] F. Han, H. Cheng, Z. Li, Q. Wang, Metall. Mater. Trans. A 36A (2005) 645–650.
[25] D.D. Radford, V.S. Deshpande, N.A. Fleck, Int. J. Impact Eng. 31 (2005) 1152–1171.
[26] H. Zhao, I. Elnasri, S. Abdennadher, Int. J. Mech. Sci. 47 (2005) 757–774.
[27] M.S. Aly, Mater. Lett. 61 (2007) 3138–3141.
[28] M. Hakamada, T. Nomura, Y. Yamada, Y. Chino, Y.Q. Chen, H. Kusuda, M. Mabuchi, Mater. Trans. 46 (2005) 1677–1680.
[29] J. Grenstedt, J. Mech. Phys. Solids 46 (1998) 29–50.
[30] T. Miyoshi, M. Itoh, S. Akiyama, A. Kitahara, Mater. Res. Soc. Symp. Proc. 521 (1998) 133–137.
[31] G.T. Gray III, ASM Handbook, vol. 8, ASM International, 2000, pp. 462–476.
[32] H. Kolsky, Stress Waves in Solids, Clarendon Press, Oxford, 1953.
[33] P.S. Follansbee, C. Frantz, J. Eng. Mater. Technol. 105 (1983) 61–66.
[34] P.S. Follansbee, in: L.E. Murr, K.P. Staudhammer, M.A. Meyer (Eds.), Metallurgical Applications of Shock-wave and High-strain-rate Phenomena, Marcel Decker, New York, 1986, pp. 451–479.